EJGE

A New Productivity Model for Fractured Horizontal Well Considering Reservoir Heterogeneity

Songgen He[a],*, Jianchun Guo[a], Yubiao Ke[b], Zhihong Zhao[a], Yuan Zhuang[b]

a. State Key Laboratory of Oil and Gas Reservoir Geology and Exploitation, Southwest Petroleum University, Chengdu, 610500, China
b. Northeast Sichuan Gas Plant, Southwest Oil and Gas Field Branch of SINOPEC, Nanchong, 637100, China
**e-mail: hesonggen917@163.com*

ABSTRACT

For heterogeneous reservoir, a new analytical model in which start-up pressure gradient (SPG) and various fracture interactions are considered is established to predict the production of fractured horizontal wells, by the use of Equivalent Wellbore Radius (EWR) and Equivalent Percolation Resistance (EPR). Furthermore, we quantitatively analyze the production influencing factors such as fracture parameters (number, conductivity, distribution) and reservoir parameters (heterogeneity, SPG) and obtain critical parameters that affect production. It is concluded that the permeability in the two side zones have a greater impact on the fractures interaction, compared with that in the middle zones. High permeability zones require higher conductivity fractures while low permeability zones require more fractures. By comparing with the classical analytical model, this model is verified effectively and practically for heterogeneous reservoir.

KEYWORDS: Heterogeneous reservoirs; Fractured horizontal well; Production analysis; Equivalent wellbore radius; Equivalent percolation resistance

INTRODUCTION

With diagenesis and differences of sedimentary microfacies, the reservoirs with low permeability have the characteristic of serious heterogeneity. Usually, fractured horizontal wells which can further expand the contact between wellbores and formations are used to develop the heterogeneous reservoir. In addition, well production becomes very sensitive to the heterogeneity when the reservoir permeability is low [1].

In recent years, the steady-state fractured horizontal well production model in which the liquid to wellbore is not only from fractures but also from perforations has been researched with the complex potential theory and superposition principle by Ning [2]. The conformal mapping method was also used to derive the steady-state production model in rectangular reservoir [3]. And for unsteady-state, according to Green function and Newman's production principle, the pressure drop function of fractured horizontal well was concluded, and a new production model coupled with wellbore pressure loss was developed by Yao et al. [4]. Another unsteady-state fractured horizontal well production

prediction model considering non-Darcy flow was built by using elliptical flow theory, as the nonlinear flow shown in tight reservoir [5]. As for experimental method, an electrolytic simulation experiment was designed according to the water and electricity resembling principle. The equi-pressure contour distribution and fracture parameters on the production of fractured horizontal well were experimentally studied under the conditions of single well and well pattern [6]. Guo et al. [7] and He et al. [8] have analyzed the heterogeneity and non-darcy effects on fracture parameters optimization based on numerical methods. For heterogeneous reservoirs, the production prediction was not accurate by using above analytical, semi-analytical and experiment methods. Because the matrix permeability in these methods was approximatively equal to the weighted average permeability of all zones. The heterogeneity had a great impact on productivity, thus the above conventional models for fractured horizontal well production analysis were not applicable.

Prats[9] was the first to introduce the concept of Equivalent Wellbore Radius(EWR) for circular reservoir. According to his results, the EWR is the function of dimensionless conductivity and half fracture length. Equivalent Percolation Resistance(EPR) was used to calculate the production in the steady-state flow [10]. In this paper, a new analytical model to analyze the production of fractured horizontal wells for heterogeneous reservoirs is obtained with EPR and an extended EWR for rectangular reservoir. With this new model, the production of fractured horizontal wells can be predicted directly and accurately, and provide the theoretical basis of production optimization for heterogeneous reservoir.

MODEL DEVELOPMENT

Physical Model

The drainage area is a parallelepiped porous medium with three kinds of permeability zone, as shown in Fig.1. Usually, the reservoirs with heterogeneity characteristic have low permeability, and hydraulic fractures are usually long and narrow, and the optimal fracture length can be as long as the width of drainage area controlled by one fractured horizontal well, which means that the fracture penetration ratio is equal to 1, according to Unified Fracture Design (UFD) for low permeability reservoirs [11].

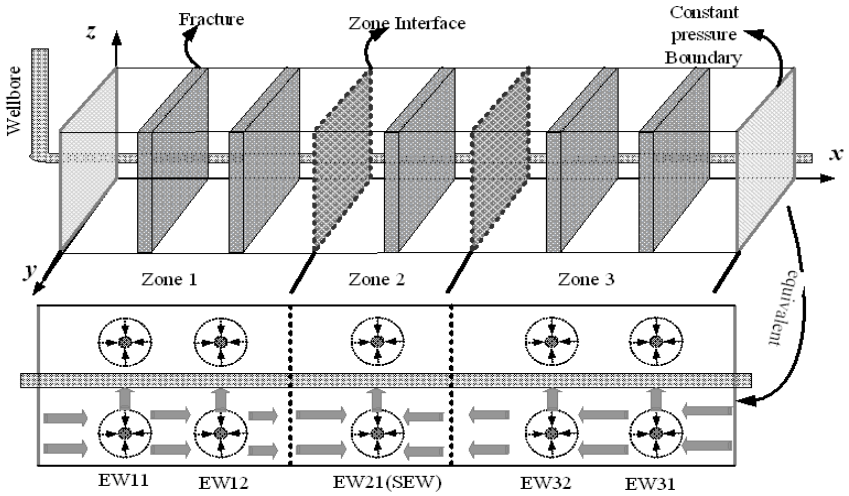

Figure 1: schematic of a fractured horizontal well in a rectangular heterogeneous reservoir(EW presents Equivalent Well, SW presents Shunt Well)

At the condition of constant pressure boundary which distribute on both sides of the reservoir, the seepage is steady-state flow. As shown in Fig.2(a), the actual flow process is that the fluid goes to fractures through matrix(region Ⅰ) in manner of linear flow, then one part of fluid goes to the horizontal wellbore through fracture(region Ⅱ and Ⅲ) in manner of linear flow and convergence flow, and another part passes through the fracture to the next matrix [12]. When each fracture is equivalent to two symmetrical, equal strength vertical wells at the direction of fracture length (y direction) with equivalent wellbore radius (EWR), the equivalent flow process is that the fluid goes to the neighborhood of fracture through matrix(region Ⅰ) in manner of linear flow, and one part goes to the equivalent well in manner of radial flow(region Ⅱ), then reaches the horizontal wellbore in manner of convergence flow(region Ⅲ), another part passes through the neighborhood of equivalent well to the next matrix, as seen in Fig.2(b). There exist one or two fractures (equivalent wells) which are called shunt fractures (shunt equivalent wells) to converge fluid from both boundaries [11].

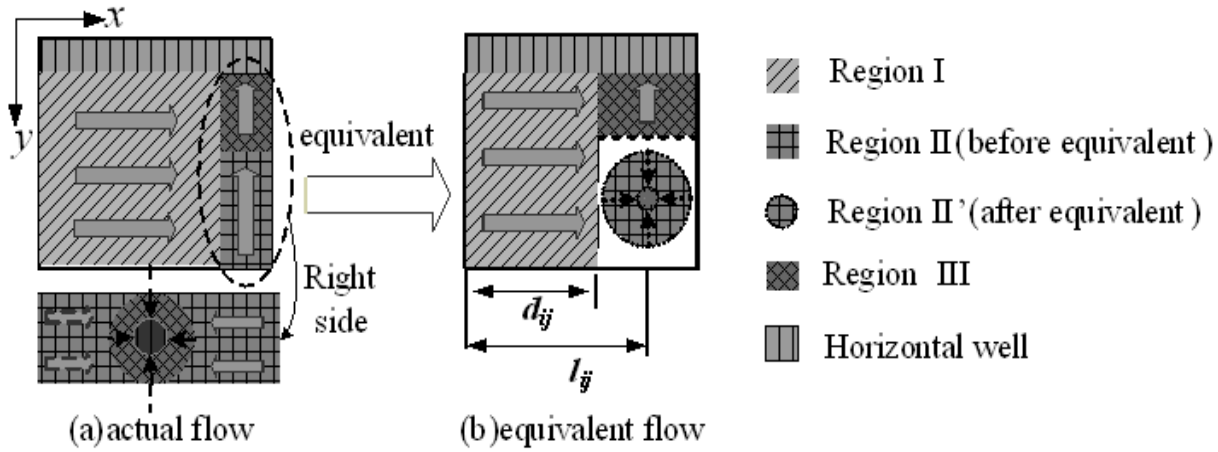

Figure 2: Equivalent schematic of seepage Unit

Mathematical Model

Calculations can be done on half of the fracture and drainage area due to the symmetric nature of the fracture and reservoir system, and there exist many similar seepage units. Before the fractures are equivalent, the seepage unit is consist of matrix linear, fracture linear and convergence flow at the junction of fracture and wellbore(Fig.2(a)), after that, it is made up of matrix linear flow in region Ⅰ, radial flow near the equivalent well in region Ⅱ, and convergence flow in region Ⅲ(Fig.2b)). So seepage resistance can be studied according to the basic flow equation firstly. Then the production of fractured horizontal well can be derived with EPR to connect each unit and its resistance based on the pressure continuity.

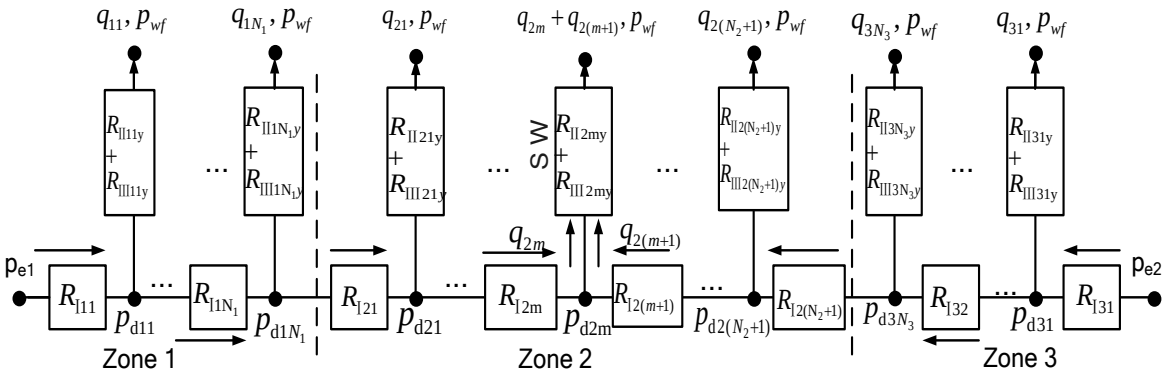

Figure 3: Equivalent schematic of half reservoir

Fracture production in the permeability zone 1 is:

$$\begin{cases} p_{e1}-p_{wf}-d_{11}G_1=\left(\sum_{j=1}^{N_1}q_{1j}+\sum_{j=1}^{m}q_{2j}\right)R_{I11}+q_{11}(R_{II11y}+R_{III11y}) \\ -d_{12}G_1=-q_{11}(R_{II11y}+R_{III11y})+\left(\sum_{j=2}^{N_1}q_{1j}+\sum_{j=1}^{m}q_{2j}\right)R_{I12}+q_{12}(R_{II12y}+R_{III12y}) \\ \cdots\cdots \\ -d_{1N_1}G_1=-q_{1(N_1\text{-}1)}(R_{II1(N_1\text{-}1)y}+R_{III1(N_1\text{-}1)y})+\left(q_{1(N_1\text{-}1)}+\sum_{j=1}^{m}q_{2j}\right)R_{I1N_1}+q_{1N_1}(R_{II1N_1y}+R_{III1N_1y}) \end{cases} \quad (1)$$

And that in the permeability zone 3 refer to equation (2):

$$\begin{cases} p_{e2}-p_{wf}-d_{31}G_3=\left(\sum_{j=1}^{N_3}q_{3j}+\sum_{j=m+1}^{N_2+1}q_{2j}\right)R_{I31}+q_{31}(R_{II31y}+R_{III31y}) \\ -d_{32}G_3=-q_{31}(R_{II31y}+R_{III31y})+\left(\sum_{j=2}^{N_3}q_{3j}+\sum_{j=m+1}^{N_2+1}q_{2j}\right)R_{I32}+q_{32}(R_{II32y}+R_{III32y}) \\ \cdots\cdots \\ -d_{3N_3}G_3=-q_{3(N_3\text{-}1)}(R_{II3(N_3\text{-}1)y}+R_{III3(N_3\text{-}1)y})+\left(q_{3N_3}+\sum_{j=m+1}^{N_2+1}q_{2j}\right)R_{I3N_3}+q_{3N_3}(R_{II3N_3y}+R_{III3N_3y}) \end{cases} \quad (2)$$

$$\begin{cases} -G_1(L_1-\sum_{j=1}^{N_1}l_{1j})-G_2d_{21}=-q_{1N_1}(R_{IIN_1y}+R_{III1N_1y})+\sum_{j=1}^{m}q_{2j}(R_{I1N_1+1}+R_{I21})+q_{21}(R_{II21y}+R_{III21y}) \\ -G_2d_{22}=-q_{21}(R_{II21y}+R_{III21y})+\sum_{j=2}^{m}q_{2j}R_{I22}+(R_{II22y}+R_{III22y}) \\ \cdots\cdots \\ -G_2d_{2m}=-q_{2(m\text{-}1)}(R_{II2(m\text{-}1)y}+R_{III2(m\text{-}1)y})+q_{2m}R_{I2m}+\left(q_{2m}+q_{2(m+1)}\right)(R_{II2my}+R_{III2my}) \\ G_2d_{2(m+1)}=-\left(q_{2m}+q_{2(m+1)}\right)(R_{II2my}+R_{III2my})-q_{2(m+1)}R_{I2(m+1)}+q_{2(m+2)}(R_{II2(m+2)y}+R_{III2(m+2)y}) \\ \cdots\cdots \\ G_2d_{2N_2}=-q_{2N_2}(R_{II2N_2y}+R_{III2N_2y})-\sum_{j=m+1}^{N_2}q_{2j}R_{I2N_2}+q_{2(N_2+1)}(R_{II2(N_2+1)y}+R_{III2(N_2+1)y}) \\ G_3(L_3-\sum_{j=1}^{N_3}l_{3j})+G_2d_{2(N_2+1)}=-q_{2(N_2+1)}(R_{II2(N_2+1)y}+R_{III2(N_2+1)y})-\sum_{j=m+1}^{N_2+1}q_{2j}(R_{I3(N_3+1)}+R_{I2(N_2+1)})+q_{3N_3}(R_{II3N_3y}+R_{III3N_3y}) \end{cases} \quad (3)$$

As to the permeability zone 2, there exist two side seepage units which connect zone 1 and zone 3 respectively, and their resistances (R_{I21} and R_{I2N2+1}) of region Ⅰ contain two parts, as well as the starting pressure (G_i). Assuming that the m equivalent wells are shunt wells which converge the fluid from both sides, so the production of fractures in the permeability zone 2 is shown as equation (3).

Because of the symmetry of the drainage area, the total production of fractured horizontal well is:

$$Q = 2\sum_{i=1}^{3}\sum_{j=1}^{N_i} q_{ij} \quad (4)$$

Model Verification

Fan had researched analytical production model for multiply fractured horizontal wells in homogeneous rectangular reservoirs with conformal mapping method [3]. Hu also obtained analytical steady-production model with Equivalent Percolation Resistance in homogeneous reservoirs [14]. As to heterogeneous rectangular reservoir, in the two classic models, the matrix permeability takes the weighted average. At the same condition (the fluid is only from fractures, the fractures are equally spaced along the horizontal well and penetrate the reservoir completely), prediction values from all models and the actual productivity value are compared at Fig.4 and Fig.5. Table 1 presents the basic parameters which from one fractured horizontal well in Da Qing [15].

Table 1: Basic Parameters (SPG represents Start-up Pressure Gradient)

Parameter	value	parameter	value
Reservoir width, $2x_f$ (m)	240	Oil volume factor, B_o	1.13
Reservoir thickness, h (m)	15	Oil viscosity, μ_o (mPa·s)	8
Horizontal well radius, r_w (m)	0.1	Fracture conductivity, D_f (D·cm)	20
Horizontal well pressure, p_{wf} (MPa)	10	Fracture number, N	5
Boundary pressure, p_e (MPa)	25		
	Zone 1	Zone 2	Zone 3
Zone length, L_i (m)	600	600	600
Matrix permeability, k_i (mD)	1	1.6	1
SPG, G_i (MPa/m)	0.01	0.0063	0.01

As shown in Fig.4 and Fig.5, with few fracture numbers and low fracture conductivity, the prediction from the new model agrees well with the two classic models. With the increase of number and conductivity, the prediction of the new model is gradually less than Hu's prediction and much less than Fan's prediction. This is due to that the starting pressure gradient and the production differences from the fractures are ignored in the classic models. Furthermore, the Fan's model doesn't consider various fracture interactions. The reservoir actual value is 31.4m3/d. it is concluded that the new model predicts more accurately. Therefore, the mew model can be applied for heterogeneous reservoir directly and has higher accuracy

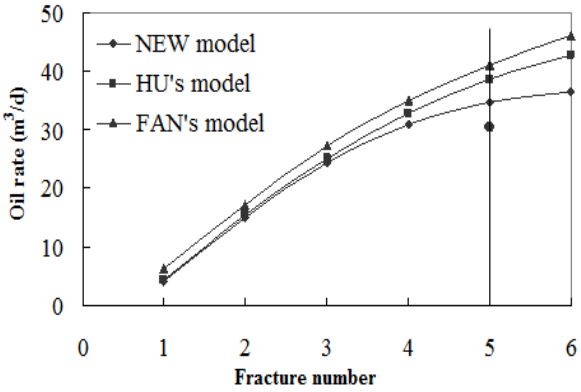

Figure 4: Well productivity vs fracture number conductivity

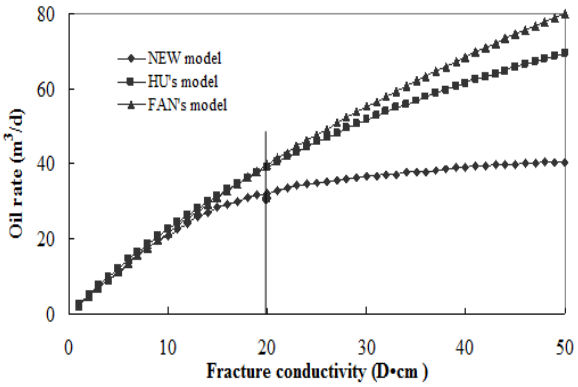

Figure 5: Productivity vs fracture

PRODUCTION ANALYSIS

In order to analyze the influencing factors of productivity, three cases whose heterogeneity characteristic was shown in Table.2 were studied. The three cases have the same weighted average matrix permeability.

Table 2: Three cases of Matrix Permeability (MP) in the Three Zones

case	Ⅰ	Ⅱ (homogeneity)	Ⅲ
MP (mD)	K_1=1 K_3=1 K_2=1.6	K_1=1.2 K_3=1.2 K_2=1.2	K_1=1.4 K_3=1.4 K_2=0.8

Productivity: finite-conductivity fractures vs infinite ones

The main difference between finite conductivity fracture productivity and infinite one is that the radial flow resistance in region Ⅱ is different. For infinite one, it ($R_{\mathrm{II}\,wij}$) for infinite one can be obtained when relative conductivity tends to infinite:

$$R_{\mathrm{II}\,wij} = R_{\mathrm{II}\,yij}(C_{FD} \to +\infty) \quad (5)$$

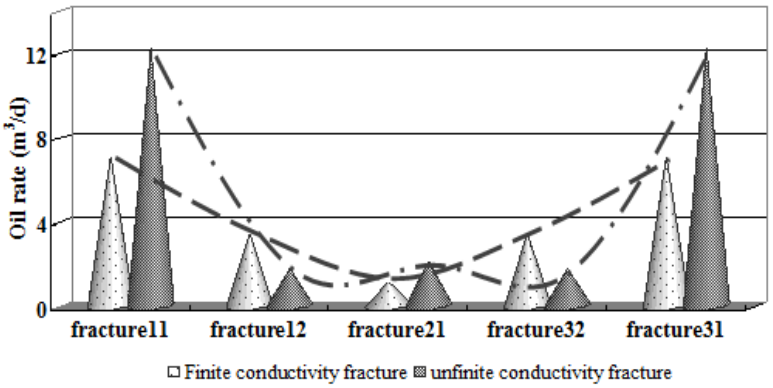

Figure 6: Fracture production difference between finite fractures and infinite ones

As shown in Fig.6, productivity from the two sides is larger than that from middle fractures. This is because the interaction of the middle fractures is more serious and drainage area of the two sides is larger. Therefore the two sides contribute more to the well productivity. This phenomenon is more obvious in infinite conductivity. Thus the flow resistance in hydraulic fracture can't be ignored generally in low permeability formation, if the fractures are taken as infinite ones, the prediction will be larger 33.4 % than the finite ones in case Ⅰ.

Productivity difference between different cases

As seen from Fig.7 and Table.3, productivity from fractures at the two side zones is larger than that from middle zone. With the increase of MP in two side zones and decrease of MP in middle zone(case Ⅰ→ case Ⅱ→ case Ⅲ), the resistance of linear flow in region Ⅰ decreases, which results in the increase of fracture productivity. But the productivity increase rate (PIR) of fracture in two side zones is less than that in central zone. Therefore it is reasonable to conclude that if the MP in two side zones is higher than that in central zone (case Ⅲ), fractures productivity difference becomes small, and it will be beneficial to uniform production profile.

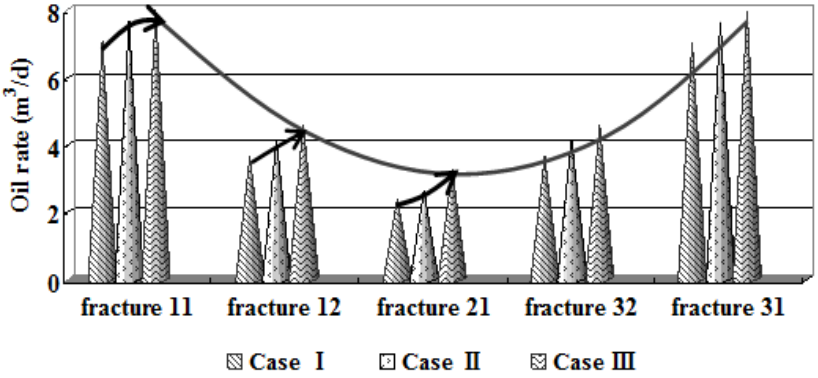

Figure 7: Fracture production difference between different cases

Table 3: PIR of different location fractures

parameter	fracture11	fracture12	fracture21	fracture32	fracture31
PIR 1 (%)	7.63	16.74	26.91	16.74	7.63
PIR 2 (%)	3.42	12.73	63.82	12.73	3.42

For fracture *ij*, PIR 1 and PIR 2 represent the fracture productivity increase rate:

$$PIR_{ij1} = \frac{q_{ijcaseII} - q_{ijcaseI}}{q_{ijcaseI}} \times 100\%$$
$$PIR_{ij2} = \frac{q_{ijcaseIII} - q_{ijcaseII}}{q_{ijcaseII}} \times 100\% \quad (6)$$

Influence of fracture number and conductivity

Fig.8 and Fig.9 present the well productivity varying with fracture number and conductivity respectively. Due to the fractures interaction, with the increase of number and conductivity, well productivity increases and the increment decreases.

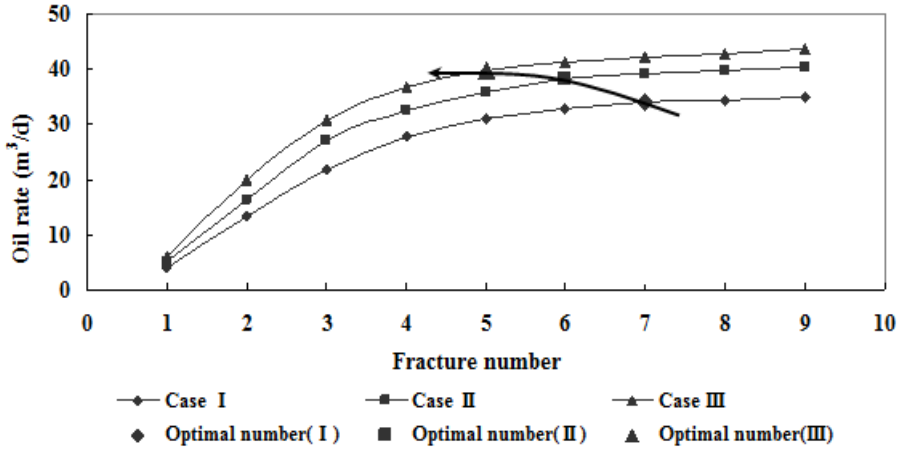

Figure 8: Productivity vs fracture number

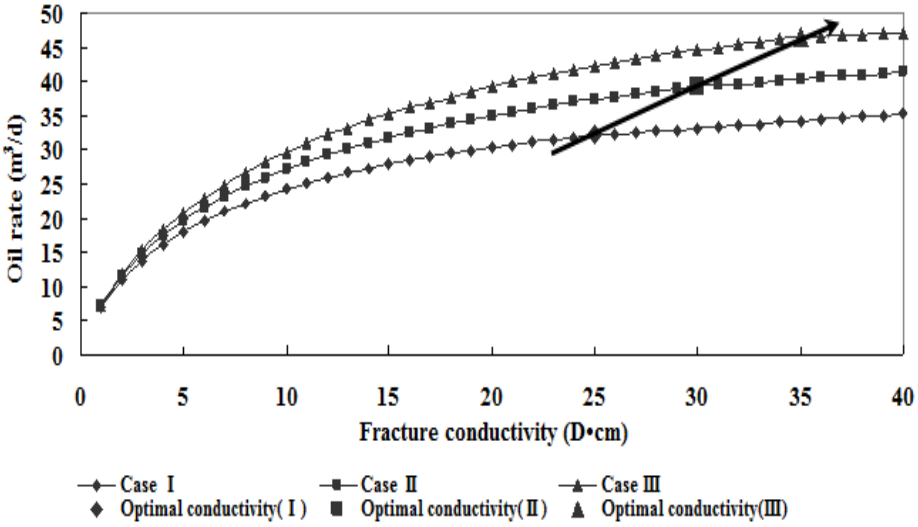

Figure 9: Productivity vs fracture conductivity

But compared with results from conventional model [14], this new model optimizes different optimal fracture parameters for different heterogeneous reservoir. The optimal number in relatively

high permeability of two side zones (case Ⅲ) is less than that in relatively low permeability of two sides (case Ⅰ). However the optimal conductivity is just the opposite. For example, the optimal number is 7 and optiaml conductivity is 25 D·cm in case Ⅰ, but the optimal number is 5 and optimal conductivity is 35 D·cm in case Ⅲ.

Influence of fracture distribution

Fracture distribution contains number distribution and conductivity distribution (Table.4). While the conductivity of fractures from all zones is the same value (20 D·cm), with the decrease of fracture number at two side zones and increase of fracture number at middle zone (number distribution 1→number distribution 2→number distribution 3), productivity decreases in case Ⅰ and increases in case Ⅲ. It means that more fracture number should be distributed at low permeability zones. In number distribution 2, with increased fracture conductivity at two side zones, the productivity of case Ⅰ decreases and case Ⅲ increases. It is because that not only high MP, but also high fracture conductivity can result in serious fractures interaction. Therefore high permeability zones need high conductivity fractures and few fracture number, and low permeability zones need low conductivity fractures and more fracture number.

Table 4: Well production under different fracture distribution

Conductivity (D·cm)	Number Distribution 1			Number Distribution 2			Number Distribution 3		
Case	I	II	III	I	II	III	I	II	III
$C_{FD1}=C_{FD3}=15$ $C_{FD2}=30$	30.8	31.7	32.1	29.4	32.1	33.9	29.2	32.6	35.6
$C_{FD1}=C_{FD3}=20$ $C_{FD2}=20$	31.3	32.6	33.2	28.1	31.2	34.3	26.7	30.2	35.3
$C_{FD1}=C_{FD3}=25$ $C_{FD2}=10$	32.2	34.3	36.1	27.7	30.4	38.2	24.2	28.3	35.2

Influence of heterogeneity

The starting pressure gradient is related to permeability, the relationship between the starting pressure gradient and matrix permeability is:

$$G_i = A\left(\frac{k_i}{\mu}\right)^{-n} \tag{7}$$

Where n=1, A is related to the media deformation coefficient (value= 0, 0.005, 0.01, 0.015, 0.02). It can be seen in Fig.10, from case Ⅰ to case Ⅲ, with the increase of production, the increment decreases gradually. But the increment of A=0 decreases faster than that of A=0.02. At the same time, with the increased A, the value of SPG, G_i, is increasing, and the production decreases. Decrement of case Ⅰ is bigger than that of case Ⅲ. This is because with larger permeability, SPG is smaller, and the effect of SPG in case Ⅲ reduce, compared with that in case Ⅰ. In other words, the interaction between fractures becomes more serious from case Ⅰ to case Ⅲ, and the two side zones have a more pronounced effect on the interaction.

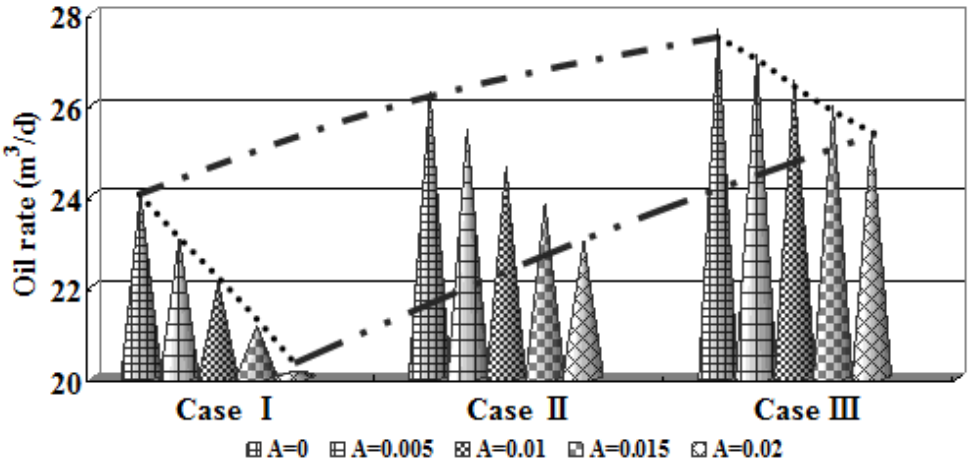

Figure 10: Histogram of well production in different heterogeneity

CONCLUSIONS

A new analytical model for productivity prediction of fractured horizontal wells in heterogeneous reservoir was developed. In this approach the Equivalent Wellbore Radius for rectangular reservoir was derived and Equivalent Percolation Resistance was used. The following conclusions could be derived.

(1) Productivity from fractures at the two side zones contributes more to the total productivity than that from intermediate fractures.

(2) For different heterogeneous characteristic, there are different optimal fracture number and conductivity. If the matrix permeability of two side zones is relatively low, the number of fractures must increase, and the average conductivity can be relatively low. The case with relatively low matrix permeability of two side zones is on the contrary.

(3) It is demonstrated that in heterogeneous rectangular reservoirs, low permeability zones need more fractures and low conductivity, while high permeability zones need fewer fractures and high conductivity.

(4) Compared with the permeability in the middle zone, the two side zones have a greater impact on the fractures interaction.

(5) The characteristic of heterogeneity had a great effect on productivity of fractured horizontal well, thus the conventional model for fracture parameters optimizing are not applicable.

APPENDIX

A. Equivalent wellbore radius for rectangular reservoir

Seepage unit *j* in zone *i* can be selected as object. The flow model can be expressed in dimensionless form through the following groups. The dimensionless distance is defined respectively by:

$$\begin{cases} x_D = \dfrac{x}{x_f} \\ y_D = \dfrac{y}{x_f} \end{cases} \quad (A.1)$$

The dimensionless distances to the unit boundaries are given by x_{eD}, y_{eD} and r_{eD}.

In this model, dimensionless fracture conductivity is defined as:

$$C_{FD} = \frac{k_f w_f}{k_i x_f} \quad (A.2)$$

The dimensionless pressure and oil rate are described as:

$$\begin{cases} p_D = \dfrac{k_i h(\mathrm{p}_u - \mathrm{p})}{141.2 q B_0 \mu} \\ G_D = C_\rho G x_f \end{cases} \quad (A.3)$$

$$q_D = \frac{x_f q_t}{q} \quad (A.4)$$

The radius of equivalent well (r_{Ew}) can be calculated by equivalent well model in rectangular reservoir and its basic idea is that the relationship between equivalent well radius (r_{Ew}) and half-length of fracture (x_f) is decided by comparing the oil rate between half fracture and equivalent vertical well.

Oil rate of vertical well

A vertical well locates at the rectangular reservoir in which there are two parallel closed boundaries and one constant pressure boundary. Through mirror reflection principle, we can get the straight injection wells row and the straight production wells row in infinite reservoir (Fig.A-1), so the potential at any point (M) in the reservoir can be obtained with conformal mapping method [13].

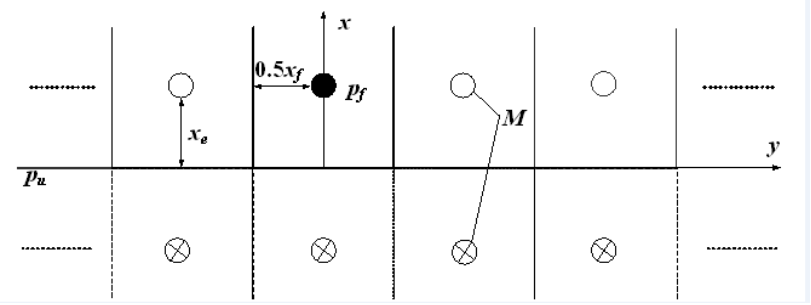

Fig.A.1 Section of mirror reflection principle

$$\Phi_M = \Phi_u + \frac{q_{\mathrm{h}}}{4\pi} \ln \frac{\mathrm{ch}\dfrac{\pi(x - x_e)}{x_f} - \cos\dfrac{\pi y}{x_f}}{\mathrm{ch}\dfrac{\pi(x + x_e)}{x_f} - \cos\dfrac{\pi y}{x_f}} \quad (A.5)$$

So the oil rate of one well in per thickness is:

$$q_{\mathrm{h}} = \frac{2\pi(\Phi_u - \Phi_f)}{\ln\frac{x_f}{\pi r_{Ew}} + \ln(2\,\mathrm{sh}\frac{\pi x_e}{x_f})} \tag{A.6}$$

The length of unit boundary (x_e) is larger than half fracture length (x_f), the value of $e^{-\frac{\pi x_e}{x_f}}$ is small enough to be ignored, then

$$\ln(2\,\mathrm{sh}\frac{\pi x_e}{x_f}) = \ln\left[2(\mathrm{e}^{\frac{\pi x_e}{x_f}} - \mathrm{e}^{-\frac{\pi x_e}{x_f}})\bullet\frac{1}{2}\right] \approx \frac{\pi x_e}{x_f} \tag{A.7}$$

Substituting A-7 into A-6, the oil rate of equivalent vertical well can be obtained as following:

$$q_{\mathrm{h}} = \frac{2\pi(\Phi_u - \Phi_f)}{\ln\frac{x_f}{\pi r_{Ew}} + \frac{\pi x_e}{x_f}} \tag{A.8}$$

$$q = \frac{p_u - p_f}{\frac{\mu B_0}{2\pi k_i h}\ln\frac{x_f}{2\pi r_{Ew}} + \frac{\mu B_0 x_e}{x_f k_i h}} \tag{A.9}$$

Oil rate of half fracture

A fracture locates at the rectangular reservoir in which there are two parallel closed boundaries and one constant pressure boundary. The half fracture diffusivity equation is [17]:

$$\begin{cases} \dfrac{\partial^2 p_{\mathrm{II}D}}{\partial y_D^2} = \dfrac{\pi}{C_{FD}} q_D(y_D) \\ \dfrac{\partial p_{\mathrm{II}D}}{\partial y_D}\Big/_{y_D=0} = -\dfrac{\pi}{C_{FD}} \\ \dfrac{\partial p_{\mathrm{II}D}}{\partial y_D}\Big/_{y_D=1} = 0 \end{cases} \tag{A.10}$$

Integrating from 0 to y_D, the equation of half fracture is:

$$\int_0^{y_D} \frac{\partial^2 p_{\mathrm{II}D}}{\partial y_D^2} dy_D = \int_0^{y_D} \frac{\pi}{C_{FD}} q_D(y_D) dy_D \tag{A.11}$$

$$\left(\frac{\partial p_{\mathrm{II}D}}{\partial y_D}\right)_{y_D=y_D} - \left(\frac{\partial p_{\mathrm{II}D}}{\partial y_D}\right)_{y_D=0} = \frac{\pi}{C_{FD}} \int_0^{y_D} q_D(y_D) dy_D \tag{A.12}$$

Using the inner boundary condition

$$\frac{\partial p_{\mathrm{II}D}}{\partial y_D} + \frac{\pi}{C_{FD}} = \frac{\pi}{C_{FD}} \int_0^{y_D} q_D(y_D) dy_D \tag{A.13}$$

Integrating from 0 to y_D, the equation is:

$$\int_0^{y_D} \frac{\partial p_{\mathrm{II}D}}{\partial y_D} dy_D + \frac{\pi}{C_{FD}} y_D = \frac{\pi}{C_{FD}} \int_0^{y_D} \int_0^{y_D} q_D(y_D) dy_D dy_D \tag{A.14}$$

$$\int_0^{y_D} dp_{\text{II}D} + \frac{\pi}{C_{FD}} y_D = \frac{\pi}{C_{FD}} y_D \int_0^{y_D} q_D(y_D) dy_D - \frac{\pi}{C_{FD}} \int_0^{y_D} y_D q_D(y_D) dy_D \quad \text{(A.15)}$$

Discrete the half-fracture in *M* equal cells, the equation is:

$$\sum_{t=1}^{s} \int_{y_{Dt-1/2}}^{y_{Dt+1/2}} dp_{\text{II}D} + \frac{\pi}{C_{FD}} y_{Ds} = \frac{\pi}{C_{FD}} y_{Ds} \sum_{t=1}^{s} q_D(y_{Dt}) \int_{y_{Dt-1/2}}^{y_{Dt+1/2}} dy_D - \frac{\pi}{C_{FD}} \sum_{t=1}^{s} q_D(y_{Dt}) \int_{y_{Dt-1/2}}^{y_{Dt+1/2}} y_{Ds} dy_D \quad \text{(A.16)}$$

$$\sum_{t=1}^{s} (p_{\text{II}D}(y_{Dt+1/2}) - p_{\text{II}D}(y_{Dt-1/2})) + \frac{\pi}{C_{FD}} y_{Ds} = \frac{\pi}{C_{FD}} y_{Ds} \sum_{t=1}^{s} q_D(y_{Dt})(y_{Dt+1/2} - y_{Dt-1/2}) - \frac{\pi}{C_{FD}} \sum_{t=1}^{s} q_D(y_{Dt}) \left(\frac{y_{Dt+1/2}^2 - y_{Dt-1/2}^2}{2} \right) \quad \text{(A.17)}$$

Defining:

$$\Delta y_D = y_{Dt+1/2} - y_{Dt-1/2} \quad \text{(A.18)}$$

$$y_{Dt+1/2} = y_{Dt} + \frac{\Delta y_D}{2}, y_{Dt-1/2} = y_{Dt} - \frac{\Delta y_D}{2} \quad \text{(A.19)}$$

Substituting A-18 and A-19 into A-17, the equation is:

$$\sum_{t=1}^{s} (p_{\text{II}D}(y_{Dt+1/2}) - p_{\text{II}D}(y_{Dt-1/2})) + \frac{\pi}{C_{FD}} y_{Ds} = \frac{\pi}{C_{FD}} y_{Ds} \Delta y_D \sum_{t=1}^{s} q_D(y_{Dt}) - \frac{\pi}{C_{FD}} \Delta y_D \sum_{t=1}^{s} q_D(y_{Dt}) y_{Dt} \quad \text{(A.20)}$$

Substituting $p_{\text{II}D}(y_{D0}) = p_{fD}$ into A-20, the half-fracture equation can be obtained as below:

$$\begin{cases} p_{\text{II}D}(y_{D1}) = p_{fD} - \frac{\pi}{C_{FD}} y_{D1} \\ p_{\text{II}D}(y_{D2}) = p_{fD} - \frac{\pi}{C_{FD}} \left(y_{D2} - \Delta y_D^2 q_D(y_{D1}) \right) \\ p_{\text{II}D}(y_{D3}) = p_{fD} - \frac{\pi}{C_{FD}} \left(y_{D3} - \Delta y_D^2 \left(q_D(y_{D1}) + q_D(y_{D2}) \right) \right) \\ p_{\text{II}D}(y_{D4}) = p_{fD} - \frac{\pi}{C_{FD}} \left(y_{D4} - \Delta y_D^2 \left(q_D(y_{D1}) + q_D(y_{D2}) + q_D(y_{D3}) \right) \right) \\ \cdots\cdots \\ p_{\text{II}D}(y_{DS}) = p_{fD} - \frac{\pi}{C_{FD}} \left(y_{DS} - \Delta y_D^2 \sum_{t=1}^{S-1} q_D(y_{Dt}) \right) \\ \cdots\cdots \\ p_{\text{II}D}(y_{DM}) = p_{fD} - \frac{\pi}{C_{FD}} \left(y_{DM} - \Delta y_D^2 \sum_{t=1}^{M-1} q_D(y_{Dt}) \right) \end{cases} \quad \text{(A.21)}$$

With the matrix linear-flow equation:

$$p_{\text{II}D}(y_{DS}) = p_{uD} - l_D q_D(y_{DS}) \quad \text{(A.22)}$$

In order to complete the system of equations, the dimensionless drop in pressure is set to unity. Matrix notation is:

$$\begin{bmatrix} l_D & 0 & 0 & 0 & \cdots & 0 \\ \frac{\pi\Delta y_D^2}{C_{FD}} & l_D & 0 & 0 & \cdots & 0 \\ \frac{\pi\Delta y_D^2}{C_{FD}} & \frac{\pi\Delta y_D^2}{C_{FD}} & l_D & 0 & \cdots & 0 \\ \frac{\pi\Delta y_D^2}{C_{FD}} & \frac{\pi\Delta y_D^2}{C_{FD}} & \frac{\pi\Delta y_D^2}{C_{FD}} & l_D & \cdots & 0 \\ \vdots & \vdots & \vdots & \vdots & \vdots & \vdots \\ \frac{\pi\Delta y_D^2}{C_{FD}} & \frac{\pi\Delta y_D^2}{C_{FD}} & \frac{\pi\Delta y_D^2}{C_{FD}} & \frac{\pi\Delta y_D^2}{C_{FD}} & \cdots & l_D \end{bmatrix} \begin{bmatrix} q_{D1} \\ q_{D2} \\ q_{D3} \\ q_{D4} \\ \vdots \\ q_{DM} \end{bmatrix} = \begin{bmatrix} p_{uD-}p_{fD} + \frac{\pi y_{D1}}{C_{FD}} \\ p_{uD-}p_{fD} + \frac{\pi y_{D2}}{C_{FD}} \\ p_{uD-}p_{fD} + \frac{\pi y_{D3}}{C_{FD}} \\ p_{uD-}p_{fD} + \frac{\pi y_{D4}}{C_{FD}} \\ \vdots \\ p_{uD-}p_{fD} + \frac{\pi y_{DM}}{C_{FD}} \end{bmatrix} \tag{A.23}$$

So the dimensionless oil rate of half fracture is obtained:

$$q_D = \lim_{M\to\infty} \sum_{t=1}^{M} q_{Dt} \tag{A.24}$$

Then the oil rate of half fracture is:

$$q = \frac{p_u - p_f}{\frac{\mu B_o l}{x_f k_i h} + \frac{\mu B_0}{3k_i h} \cdot \frac{1.65 - 0.328\ln C_{FD} + 0.116(\ln C_{FD})^2}{1 + 0.18\ln C_{FD} + 0.064(\ln C_{FD})^2 + 0.005(\ln C_{FD})^3}} \tag{A.25}$$

Comparing the oil rate between half fracture and equivalent vertical well, the radius of equivalent vertical well in rectangular reservoir is:

$$r_{Ew} = \frac{x_f}{2\pi}\exp\left(-\frac{1}{2} - \frac{2\pi}{3}\frac{1.65 - 0.328\ln C_{FD} + 0.116(\ln C_{FD})^2}{1 + 0.18\ln C_{FD} + 0.064(\ln C_{FD})^2 + 0.005(\ln C_{FD})^3}\right) \tag{A.26}$$

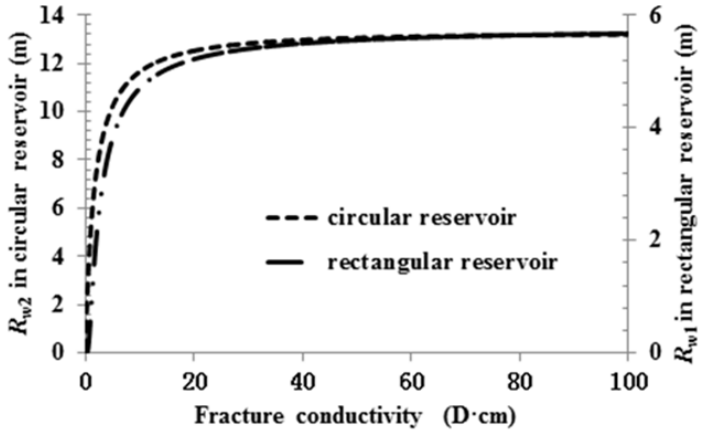

Fig.A.2 The relationship between equivalent wellbore radius and fracture conductivity

The relation curve between equivalent wellbore radius and fracture conductivity is shown in Fig.A.2, with increase of fracture conductivity, equivalent wellbore radius in rectangular reservoir increases but the increase rate slows down. When the conductivity reaches 20D·cm, the rate is close to zero. The trend is similar to that of equivalent wellbore radius in circular reservoir [16]. It can be concluded that the new equivalent wellbore model in rectangular reservoir has good accuracy. The radius of equivalent wellbore in circular reservoir is approximately twice larger than that in

rectangular reservoir. Because one fracture is equivalent to one vertical well in circular reservoir and one fracture is equivalent to two symmetrical, equal strength vertical wells in rectangular reservoir.

B. calculation of flow resistance

Resistance in region Ⅰ

Considering start-pressure gradient, the diffusivity equation in region Ⅰ is [17]:

$$\begin{cases} \dfrac{\partial^2 p_{\mathrm{I}D}}{\partial x_D^2} - G_D \dfrac{\partial p_{\mathrm{I}D}}{\partial x_D} = 0 \\ p_{\mathrm{I}D|x_D=0} = p_{uD} \\ p_{\mathrm{I}D|x_D=x_{eD}} = p_{dD} \end{cases} \tag{B.1}$$

Because of the equivalent radial drainage area, the length of linear flow in region Ⅰ (x_{ijeD}) is less than the distance between adjacent cracks (l_{ijD}), and the radial drainage perimeter is approximately equal to half fracture, so the length of linear flow is:

$$x_{eD} = l_D - \frac{1}{4\pi} \tag{B.2}$$

With Eq.B-2, the relationship between flux and pressure is:

$$p_{\mathrm{u}} - p_{\mathrm{d}} - G_i(l - \frac{x_f}{4\pi}) = q\frac{\mu B_o (l - \frac{x_f}{4\pi})}{x_{\mathrm{f}} k_i h} \tag{B.3}$$

According to Eq.B.3, we can get the linear resistance in region Ⅰ:

$$R_{\mathrm{I}} = \frac{uB_{\mathrm{o}}\left(l - \frac{x_{\mathrm{f}}}{4\pi}\right)}{\mathrm{x_f} k_i h} \tag{B.4}$$

Resistance in region Ⅱ

By the continuity of pressure, the external pressure of radial flow in region Ⅱ is equal to the internal pressure of linear flow in region Ⅰ, the diffusivity equation is given:

$$\begin{cases} \dfrac{\partial^2 p_{\mathrm{II}D}}{\partial r_D^2} + \dfrac{1}{r_D}\dfrac{\partial p_{\mathrm{II}D}}{\partial r_D} = 0 \\ p_{\mathrm{II}D|r_D=1} = p_{fD} \\ p_{\mathrm{II}D|r_D=r_{eD}} = p_{dD} \end{cases} \tag{B.5}$$

Where the drainage radius of radial flow in region Ⅱ is [13]:

$$\begin{cases} r_e = \dfrac{x_f}{2\pi} \\ r_{eD} = \dfrac{1}{2\pi} \end{cases} \tag{B.6}$$

With Eq.B-6, the relationship between the flux and the pressure in region Ⅱ is

$$p_{\mathrm{d}} - p_{\mathrm{f}} = q\frac{\mu B_{\mathrm{o}} \ln(x_{\mathrm{f}}/2\pi r_{\mathrm{w}})}{2\pi k_i h} \tag{B.7}$$

Substituting Eq.A-28 into Eq.B-7, we can obtain the approximate radial flow resistance for finite-conductivity in region Ⅱ:

$$R_{\mathrm{II\,y}} = \frac{\mu B_0}{3k_i h}\frac{1.65 - 0.328\ln C_{FD} + 0.116(\ln C_{FD})^2}{1 + 0.18\ln C_{FD} + 0.064(\ln C_{FD})^2 + 0.005(\ln C_{FD})^3} + \frac{\mu B_0}{4\pi k_i h} \tag{B.8}$$

As the same with finite-conductivity, the radial flow resistance for infinite-conductivity is:

$$R_{\mathrm{II\,w}} = \frac{\mu B_0}{4\pi k_i h} \tag{B.9}$$

Resistance in region Ⅲ

The linear flow within the hydraulic fracture is equivalent to radial flow near the equivalent well, the radial convergence of flow toward the wellbore within the hydraulic fracture can't be ignored, and the relationship between the flux and the pressure in the junction of fracture and wellbore is [18]:

$$p_{\mathrm{f}} - p_{\mathrm{wf}} = \frac{q\mu B_0(\ln\frac{h}{2r_{\mathrm{w}}} - \frac{\pi}{2})}{2\pi k_{\mathrm{f}} w_{\mathrm{f}}} \tag{B.10}$$

Due to the symmetry of reservoir, the convergence flow resistance in region Ⅲ is:

$$R_{\mathrm{III\,y}} = \frac{\mu B_{\mathrm{o}}(\ln h/2r_{\mathrm{w}} - \pi/2)}{4\pi k_{\mathrm{f}} w_{\mathrm{f}}} \tag{B.11}$$

Nomenclature

i,j: seepage unit *j* in zone *i*	*L*i: zone i length,m
p_{uij}: external pressure of linear flow in region Ⅰ, MPa	d_{ij}: length of region Ⅰ, m
p_{dij} :internal pressure of linear flow in region Ⅰ, (external pressure of radial flow in region Ⅱ), MPa	*N* : Total fracture number, dimensionless
p_{fij}: external pressure of convergence flow in region Ⅲ, (internal pressure of radial flow in region Ⅱ), MPa	N_{i} :fracture number of zone i, dimensionless
p_{wf}: pressure in horizontal wellbore,MPa	r_{e}: drainage radius of radial flow in region Ⅱ, m
p_{e1}, p_{e2}: pressure in side boundaries,MPa	x_{f}: half fracture length (reservoir width), m
$p_{\mathrm{Ⅰ}}$:pressure in region Ⅰ, MPa	w_{f}: fracture width, m
$p_{\mathrm{Ⅱ}}$:pressure in region Ⅱ, MPa	r_{w}: horizontal well radius, m
$p_{\mathrm{Ⅲ}}$:pressure in region Ⅲ, MPa	r_{Ew}: equivalent vertical well radius, m
G_{i}: start-pressure gradient in zone *i* (SPG), MPa/m	q_{ij}: flux of equivalent well, m^3/d
k_{i}: marrix permeability in zone i, mD	q_{m}: flux of shunt well, m^3/d
k_{f} :fracture permeability, D	*Q*: production of fractured horizontal well, m^3/d
μ: oil viscosity, mPa·s	$R_{\mathrm{Ⅰ\,ij}}$: flow resistance in region Ⅰ, MPa/(m^3/d)

B_o: oil volume factor, dimensionless	$R_{\text{II}ijy}$: flow resistance for finite-conductivity fracture in region Ⅱ, MPa/(m^3/d)
D_f: fracture conductivity, D·cm	$R_{\text{II}ijw}$: flow resistance for infinite-conductivity fracture in region Ⅱ,MPa/(m^3/d)
h: pay-zone thickness,m	$R_{\text{III}ij}$: flow resistance in region Ⅲ,MPa/(m^3/d)

REFERENCES

[1] Liu S., Guo H., Wang J., Chen Y., Li J.(2015) "The Geologic Condition and Fracturing Technique of Tight Sand Gas Reservoir in Xujiahe Formation" *Electronic Journal of Geotechnical Engineering*, 13465-13476.

[2] Ning Z., Han S., Cheng L.(2002) "Method for Calculating Capacity of Fractured Horizontal Wells in Low Permeability Reservoirs". *Acta Petrol Sinica*, 23(2): 68-71.

[3] Fan Z., Fang H.(1996) "The research of formula in fractured horizontal well steady-state solution". *Petroleum Exploration and Development*, 23(3):52-56.

[4] Yao, S., Zeng, F., Liu, H., Zhao, G. (2013). "A semi-analytical model for multi-stage fractured horizontal wells". *Journal of Hydrology*, 507(12), 201-212.

[5] Xiao, Q., Yang Z., Luo, Y., Wang, X. (2014). "Nonlinear flow characteristics of tight reservoir". Electronic Journal of Geotechnical Engineering, 19, 1491-1497.

[6] Wu X., Sui X., An Y.(2009) "Electrolytic simulation experiment of fractured horizontal well". *Acta Petrol Sinica*, 30(5): 740-743.

[7] Guo, J., He, S., Deng, Y. (2015). "Single-well design benefits low-permeability reservoirs". *Oil & Gas Journal*, 113(8), 39-43.

[8] He, S., Deng, Y., Guo, J., Xiao, Y., Zhao, Z. (2015). "Optimization of Staged-Fracturing in Heterogeneous Tight Gas Reservoirs of Western-Sichuan Gas Field". *SPE/IATMI Asia Pacific Oil & Gas Conference and Exhibition*. SPE176145.

[9] Prats M., Levine J.(1961) "Effect of vertical fractures on reservoir behavior-incompressible fluid case". *SPEJ*, 1(2): 105-118, SPE-1575-G.

[10] Giger F.(1985) "Horizontal wells production techniques in heterogeneous reservoir" *The Middle East Oil Technical Conference and exhibition*, SPE-13710.

[11] Bhattacharya, S., Nikolaou, M., & Economides, M. J. (2012). "Unified fracture design for very low permeability reservoirs". *Journal of Natural Gas Science & Engineering*, 9(6), 184–195.

[12] Mukherjee, H., & Economides, M. J. (1991). "A parametric comparison of horizontal and vertical well performance". *SPE Formation Evaluation*, 6(2), 209-216.

[13] Zhu, D., Yang, Z., Wang, X., & Liao, Z. (2013). "New productivity evaluation model for segregated fracturing horizontal well in low permeability and tight reservoir". *Electronic Journal of Geotechnical Engineering*, 18, 5981-5992.

[14] Hu J., Zheng Q., Zhao S.(1996) "A new method to predict performance of fractured horizontal wells". *The SPE international conference on Horizontal well technology*, SPE-37051

[15] Wan R.(1997) "Horizontal wells technology from different type reservoirs in china". *Bei*

Jing, China: Petroleum Industry Press.

[16] Wang X., Li G., Wang F.(2010) "Productivity analysis of horizontal wells intercepted by multiple finite-conductivity fractures". *Petroleum Science*, 367-371.

[17] Brown, M. L., Ozkan, E., Raghavan, R. S., & Kazemi, H. (2011). "Practical solutions for pressure-transient responses of fractured horizontal wells in unconventional shale reservoirs". *SPE Reservoir Evaluation & Engineering*, 14(6), 663-676.

[18] Mukherjee, H., & Economides, M. J. (1991). "A parametric comparison of horizontal and vertical well performance". *SPE Formation Evaluation*, 6(2), 209-216.

Editor's note.
This paper may be referred to, in other articles, as:

Songgen Hea, Jianchun Guo, Yubiao Ke, Zhihong Zhao, Yuan Zhuang: "A New Productivity Model for Fractured Horizontal Well Considering Reservoir Heterogeneity" *Electronic Journal of Geotechnical Engineering*, 2017 (22.01), pp 101-118. Available at ejge.com.